

# Sensor Selection and Motion Planning in Robotic Sensor Networks Under Communication Constraints

Abubakr Muhammad  
School of Computer Science  
McGill University, Montreal, Canada  
abubakr@cs.mcgill.ca

**Abstract**— We compare the configuration spaces corresponding to various arrangements of sensors on a robotic sensor network of three agents under the constraints of collision avoidance and maintenance of communication. We argue for the superiority of one particular sensor arrangement from the point of view of hardware complexity. This configuration space has the topology of a solid double torus. Various techniques of hyperbolic geometry and algebraic topology have been employed for motion planning on this configuration space.

## I. INTRODUCTION

Robotic multi-agent systems are an emerging application of networked sensing and control. One of the main challenges in the efficient design and implementation of these systems is the effective modeling and analysis of sensory and communication limitations of the hardware. Moreover, a systematic comparison of the performance of various sensing and communication modalities in real systems is also required.

In this paper, we study the problem of motion planning in a robotic sensor network under various sensor arrangements for detecting collision and maintenance of communication. By a sensor arrangement, we mean a particular configuration of possibly heterogenous sensors for detecting collisions and for the maintenance of all-to-all communication. We emphasize that different choices of sensor arrangements give rise to different configuration spaces, some of which have non-trivial topologies. We also note that some sensor arrangements enable motion planning with a lesser hardware complexity and communication cost. Our ultimate goal is to study this problem for an arbitrary number of agents and to construct proper navigation functions constructively. The price to pay for this hardware simplicity is a relatively complex motion planning algorithm on a non-trivial configuration space. In this paper, we have restricted ourselves to the case of three agents. We shall see later that even for three agents, the configuration spaces arising from the constraints have interesting topological and geometrical features. It is hoped that the techniques developed here give clues to the solution of this problem for bigger networks.

The systematic comparison of sensor arrangements for an arbitrary number of agents is still an open problem. Some attempts have been made along these lines [1], [2] from the point of view of minimal sensing and information spaces. However, much needs to be done that incorporates

communication, sensing and hardware complexity in this comparison.

The outline of this paper is as follows. In Section II, we compare and contrast the configuration spaces for various sensor arrangements on three agents. We explain the merits of one particular sensor arrangement, whose configuration space has the topology of a solid double torus. In Section III, we explicitly construct the universal covering space of the solid double torus. Moreover, we describe explicit maps that project the geodesics in the universal cover to the configuration space. Finally, we present our conclusions in Section IV.

## II. SENSOR ARRANGEMENTS AND CONFIGURATION SPACES

Consider a robotic network of  $n$  agents in a plane, whose positions are given by  $\mathbf{p}_1, \dots, \mathbf{p}_n \in \mathbb{R}^2$ . Each agent obeys the simple kinematic model  $\dot{\mathbf{p}}_i = u_i$ , where  $u_i$  is the control input for actuation in each axis of the plane. Let these agents be equipped with identical omnidirectional radios, so that each agent can communicate with other agents within a communication radius  $R_c$ . The value of  $R_c$  is limited by the minimum signal-to-noise ratio at which the radios can receive messages successfully.

A basic requirements of this robotic network is to move between different configurations while each agent maintains contact with all other agents at all times. In other words, the connectivity graph of this network is required to be complete at all times. The full connectivity implies that a message broadcast by any agent is heard simultaneously by all other agents and no more than one agents can broadcast messages at the same time.

The full connectivity of the network is only valid for a proper subset of all possible configurations. Furthermore, assume that each robot has a collision radius  $R_o/2$ , which may correspond to the largest physical dimension of a robots in the plane. It is reasonable to assume that  $R_o \ll R_c$ . Therefore, we study the set of configurations  $\mathcal{C}^n \subset (\mathbb{R}^2)^n$  that obey for all  $1 \leq i < j \leq n$ ,

- 1) the communications constraints,  $\|\mathbf{p}_i - \mathbf{p}_j\| < R_c$ ;
- 2) and the collision constraints,  $\|\mathbf{p}_i - \mathbf{p}_j\| > R_o$ .

### A. Sensor Arrangements

In order to do planning in  $\mathcal{C}^n$ , we equip each agent with a suite of sensors that helps compute the relative positions of the agents with respect to each other and detects the communication and collision constraints. The set of sensors given to each agent need not be identical. We call this hardware setup a *sensor arrangement* on the robotic network. More formally, we give the following definition.

*Definition 2.1:* For a network of  $n$  identical agents, each with a physical dimension  $R_0/2$  and a communication radius  $R_c$ , a *sensor arrangement* is a suite of  $k$  sensors fitted on possibly different agents, such that for any given  $\mathbf{p} \in \mathcal{C}^n$  and for each individual constraint on communication or collision  $f_i(\mathbf{p}) < 0$ , there exists a function  $g_i$  such that

$$g_i(\Theta(\mathbf{p})) = f_i(\mathbf{p}),$$

where  $\Theta(\mathbf{p})$  is a tuple of all sensory measurements from  $k$  sensors, measured at positions  $\mathbf{p}$ .

Thus the purpose of a sensor arrangement is to detect and quantify the satisfaction of constraints while maintaining full connectivity. A simple protocol can be used to detect network connectivity. Each agent broadcasts its unique identification tag in some pre-determined order. If after each round of broadcasts, every agent has successfully received  $n - 1$  broadcasts at its turn, the connectivity of the network is full.

Although the sensors are distinguished from the communication radios, nevertheless the radio signals can be used as a (mostly unreliable) sensory input for deducing the relative position of a transmitter from the strength of the received signal. Finally, observe that the sensors need not measure the absolute positions of the agents as we only need relevant positions for collision avoidance or maintenance of communication.

### B. Sensor Arrangements for three agents

In this paper, we restrict ourselves to the case of three agents and study the merits and demerits of different sensor arrangements for this case. We also study the geometrical and topological properties of  $\mathcal{C}_{sa}^n$  for various sensor arrangements.

1) *Two range sensors on two agents:* One arrangement could be a set of range sensors (with a longer sensory range than the communication radius  $R_c$ ), fitted on two or more agents that detect the distances  $r_1 = \|\mathbf{p}_2 - \mathbf{p}_3\|$ ,  $r_2 = \|\mathbf{p}_1 - \mathbf{p}_3\|$ ,  $r_3 = \|\mathbf{p}_1 - \mathbf{p}_2\|$  directly. Note, that we only need two range sensors on any two agents, since the presence of a range sensor on an agent implies that it can detect distances from all of its neighbors.

The constraints imply that the measured quantities should be in the range  $R_o < r_i < R_c$ . Denote by  $\mathcal{R}$  the set of all such triplets. It can be easily seen that  $\mathcal{R}$  is not a simple direct product of three open intervals,  $(R_o, R_c)^3$ . As an example, consider the triplet  $(R_c - \epsilon, R_o + \epsilon, R_o + \epsilon)$ , where  $\epsilon > 0$  is small. Let us fix  $r_1, r_2$  and see how much  $r_3$  can vary over  $(R_o, R_c)$ . It is easy to see that  $r_3$  can take a maximum value of  $\min\{R_c, r_1 + r_2\}$  and a minimum value

of  $\max\{R_o, |r_1 - r_2|\}$ . By symmetry, this implies that the configuration space is bounded by nine planar constraints,

$$\begin{aligned} r_1 < R_c, \quad r_2 < R_c, \quad r_3 < R_c, \\ r_1 > R_o, \quad r_2 > R_o, \quad r_3 > R_o, \\ r_1 + r_2 - r_3 < 0, \\ r_1 - r_2 - r_3 < 0, \\ r_1 - r_2 + r_3 < 0. \end{aligned}$$

One such space has been drawn in Figure 1. It is quite clear that this space is topologically trivial, i.e. contractible and has no topological obstacles to global navigation.

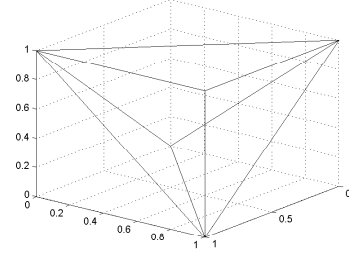


Fig. 1. The configuration space  $\mathcal{R}$  for  $R_c = 1$  and  $R_o \ll R_c$ .

2) *One range and one bearing sensor on one agent:* In another arrangement, we can equip one agent with one range and one bearing sensor. Suppose that both sensors have been fitted on agent 3 and they measure the distances  $r_1 = \|\mathbf{p}_2 - \mathbf{p}_3\|$ ,  $r_2 = \|\mathbf{p}_1 - \mathbf{p}_3\|$ , and bearing

$$\theta = \cos^{-1} \frac{(\mathbf{p}_2 - \mathbf{p}_3)^T (\mathbf{p}_1 - \mathbf{p}_3)}{\|\mathbf{p}_2 - \mathbf{p}_3\| \|\mathbf{p}_1 - \mathbf{p}_3\|}.$$

Similarly, other range and bearing measurements are obtained if the sensors are fitted on a different agent. The missing distance  $r_3$  can be recovered from this data using the law of cosines,  $r_3^2 = r_1^2 + r_2^2 - 2r_1r_2 \cos(\theta)$ . The collision constraints are translated to  $r_1, r_2 > 2R_o$ , and

$$r_1^2 + r_2^2 - 2r_1r_2 \cos(\theta) > 4R_o^2. \quad (1)$$

For the communication constraints, we need  $r_1, r_2 < R_c$ , along with

$$r_1^2 + r_2^2 - 2r_1r_2 \cos(\theta) < R_c^2. \quad (2)$$

We denote the set of all such valid triplets of bearing, range and range measurements as  $\mathcal{T}$ . Let us try to visualize this space in the coordinates  $(r_1, r_2, \theta)$ .

Let  $\theta$  vary between  $-\pi$  and  $\pi$ . Then the configuration space can be visualized as a set in  $\mathbb{R}^3$  bounded by the linear constraints  $r_1 > R_o$ ,  $r_1 < R_c$ ,  $r_2 < R_o$ ,  $r_2 < R_c$ ,  $\theta \geq -\pi$  and  $\theta \leq \pi$ . The communication and collision constraints erode this set further. Let us see how the communication constraints come into action for a fixed  $\theta$ . From (2),

$$\cos(\theta) > \frac{r_1^2 + r_2^2 - R_c^2}{2r_1r_2}.$$

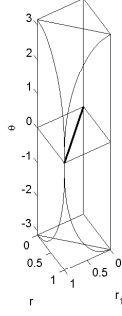


Fig. 2. The configuration space  $\mathcal{T}$  for  $R_c = 1$  and  $R_o \ll R_c$ . The planes  $\theta = \pi$  and  $\theta = -\pi$  are identified. The thick line in the plane  $\theta = 0$  depicts the collision constraint for small  $\theta$ .

Therefore  $\cos(\theta)$  serves as an upper bound for all choices of valid  $r_1, r_2$ . When  $\theta \in [-\pi/3, \pi/3]$ ,  $\cos(\theta) \leq 1/2$ . Therefore,  $r_1^2 + r_2^2 - r_1 r_2 < R_c^2$ .

This inequality is satisfied for all pairs  $r_1, r_2 < R_c$ . Therefore for  $\theta \in [-\pi/3, \pi/3]$ , all  $r_1, r_2 \in (R_o, R_c)$  satisfy the communication constraints. For  $\theta$  outside this range, this is no longer true. For example, for  $\theta = \pi/2$ , the constraint becomes  $r_1^2 + r_2^2 < R_c^2$ . The valid pairs  $r_1, r_2$  are within this disk. For the extreme case of  $\theta = \pi$ , we have  $r_1 + r_2 \leq R_c$ , which is a linear constraint.

For collision, first consider the case when  $\theta = 0$ . Inequality (1) implies that all valid range pairs satisfy  $|r_1 - r_2| > 2R_o$ . For  $\theta$  large enough, it is easy to see that the absolute difference between  $r_1$  and  $r_2$  makes no difference. Therefore, to find the cutoff value of  $\theta$  at which this constraint vanishes, let  $r_1 = r_2 = r$ , so that,

$$\cos(\theta) < 1 - 2 \left( \frac{R_o}{r} \right)^2.$$

If we let  $r \rightarrow R_c$  to maximize the right hand side of this inequality, we have the cutoff angle

$$\theta_o = \cos^{-1} \left( 1 - 2 \left( \frac{R_o}{R_c} \right)^2 \right).$$

The result is a cylindrical void in the configuration space whose axis is  $r_1 = r_2$  in the  $\theta = 0$  plane. These observations have been illustrated in Figure 2 for a special case of  $R_o$  and  $R_c$ .

Let us now analyze the topology of this configuration space. It is clear that the plane  $\theta = -\pi$  is identified with the plane  $\theta = \pi$  which creates a hole in the configuration space. If there were no other holes, the resulting space would have the topology of a solid torus. The collision constraint in (1) introduces another hole in the space via the cylindrical void mentioned above. Clearly, the two holes do not merge. We therefore have a configuration space which is homeomorphic to the interior of a *solid double torus* denoted by  $\mathbf{T}^2$  (See Figure 3). Note that this is different from the standard double torus which is a surface with hollow interior. This space has the homotopy type of a wedge sum of two circle  $S^1 \vee S^1$  (See Figure 4).

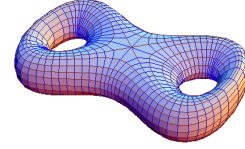


Fig. 3. The double torus as a surface in  $\mathbb{R}^3$ . By the solid double torus  $\mathbf{T}^2$ , we mean the interior of this surface.

3) *Other arrangements*: The most direct method of implementing a motion planning scheme on  $\mathcal{C}^3$  would be to have a sensor arrangement that gives direct measurement of the absolute positions of the agents, i.e. equip each agent with a GPS device. These positions can be subsequently shared with the neighbors to detect the constraints. The set of constraint-satisfying positions in this sensor arrangement is the space  $\mathcal{C}^3$  itself.

Topologically, this configuration space is similar to the standard configuration space of three points in a plane, namely,  $\mathcal{C}^3(\mathbb{R}^2) = (\mathbb{R}^2 \times \mathbb{R}^2 \times \mathbb{R}^2) \setminus \Delta$ , where  $\Delta = \{(\mathbf{p}_1, \mathbf{p}_2, \mathbf{p}_3) : \mathbf{p}_1 \neq \mathbf{p}_2, \mathbf{p}_1 \neq \mathbf{p}_3, \mathbf{p}_3 \neq \mathbf{p}_2\}$ . In this idealization, the agents are assumed to have a point-dimension and the issue of communication (or sensory) constraints between the agents is ignored.

There can also be other sensor arrangements based on a combination of relative (range, bearing) and absolute (GPS) sensors. Most research involving trajectory generation for robotic networks implicitly assumes either the configuration space  $\mathcal{C}^3(\mathbb{R}^2)$  by ignoring sensory/communication constraints or the space  $\mathcal{R}$  due to its topological simplicity. These idealizations however come at the cost of ignoring physical limitations as well as issues in economy such as hardware complexity and communication bandwidth.

We note that for the case of 3 agents, the sensor arrangement corresponding to the space  $\mathcal{T}$  not only captures the collision and communication constraints of the system, but is also more *economical* than other sensor arrangements that can be realized by other permutations of GPS, bearing and range sensors. Not only does this arrangement require only two sensors, but due to the availability of complete information on one agent, the other agents can be remotely actuated by this master agent, using a simple broadcast strategy whose frequency is only limited by the bandwidth available in the radios. In the case of  $\mathcal{R}$ , the measurements have to be communicated to other agents, which requires at least two broadcasts per set of measurements. Thus the bandwidth used in this case is doubled. In the case of the sensor arrangement with 3 GPS sensors, three rounds of broadcasts are needed before all three agents are cognizant of the global picture, and at least two broadcasts are needed for at least one agent to be knowledgeable of all three positions. In either case, this is more expensive than the arrangement corresponding to  $\mathcal{T}$ . It is easy to see that this economy extends to the case of  $n$  agents.

The price to pay for this economy is a relatively compli-

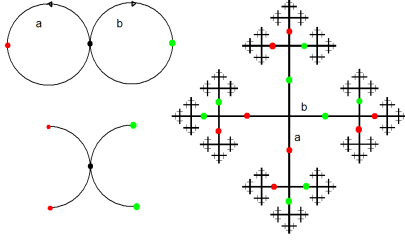


Fig. 4. The universal cover (right) of  $S^1 \vee S^1$  (top left). The fundamental domain (bottom left) is obtained after cutting the space at the green and red points. The fundamental domain is then repeatedly glued at these identification points to get the universal cover.

cated motion planning algorithm. Since the the configuration space  $\mathcal{T}$  in topologically nontrivial, a relatively complicated scheme is needed to obtain trajectories on this space. We present such a scheme in the following sections.

### III. MOTION PLANNING ON THE SOLID DOUBLE TORUS

The motion planning problem corresponds to constructing a method, which takes two configurations  $x_o, x_f$  in  $\mathcal{C}$  as an input and produces as an output a continuous trajectory that starts at  $x_o$  and ends at  $x_f$ . One approach towards obtaining such paths is to study the geodesics on  $\mathcal{C}$ . However, depending on the topology of the space, there can be a number of geodesics between any two points. It is well known that the presence of holes in a configuration space in an obstruction towards obtaining a stable motion planner, where by stability we mean that a small perturbation in the end points does not create a large variation in the geodesics. Moreover, it is usually hard to compute geodesics directly on a  $\mathcal{C}$  with complicated topology due to the absence of a trivial parametrization.

In order to do motion planning on such nontrivial configuration space, one method is to obtain a universal cover of the configuration space, which is easily parameterizable. Examples include the standard simply connected spaces such as the Euclidean spaces, unit-spheres and hyperbolic spaces. Being a local property, the geodesics can be lifted to the universal cover. The initial and final configurations are also lifted to the fundamental domain. By tracing the orbits of one of these points, several geodesics can be obtained that connect these pre-images of the covering map. Any one these geodesics, when projected down on configuration space gives a valid trajectory for motion planning. The main ingredients of this methods are explicitly constructing the universal cover and the covering maps. We now employ this method for the case of the configuration space  $\mathcal{T}$ .

#### A. Universal Cover of the Solid Double Torus

The universal cover of the solid double torus  $\mathbf{T}^2$  can be constructed by using the standard technique [3] described in Figure 4. Recall that  $\mathbf{T}^2$  has the same homotopy type as that of  $S^1 \vee S^1$ . From Figures 3 and 4, it can be seen that  $\mathbf{T}^2$  is a thickening of  $S^1 \vee S^1$ . Therefore,  $\pi_1(\mathbf{T}^2) \cong \pi_1(S^1 \vee S^1) \cong \mathbb{Z} * \mathbb{Z}$ . If  $\tilde{X}$  is the universal cover of  $\mathbf{T}^2$ , then the solid double

torus can be described as a quotient space  $\tilde{X}/(\mathbb{Z} * \mathbb{Z})$ , where the (free) group actions are described by certain isometries of the fundamental domain of  $\tilde{X}$ . In fact, the universal cover is just a thickening of the universal cover of  $S^1 \vee S^1$ .

As mentioned above, the configuration space  $\mathcal{T}$  is homeomorphic to  $\mathbf{T}^2$ . Therefore, we explicitly construct the universal cover of  $\mathbf{T}^2$  and consequently the necessary homeomorphisms. We emphasize that the particular construction explained below will be convenient for the computation of geodesics.

#### 1) Hyperbolic geometry and Mobius transformations:

We take a brief digression into hyperbolic geometry and its group of isometries called Mobius transformations. A hyperbolic geometry  $H^n$  of dimension  $n$ , satisfies all of Euclid's postulates except the parallel postulate [5]. In hyperbolic geometry, the sum of angles of a triangle is less than 180 degrees, and triangles with the same angles have the same areas.  $H^n$  has a constant (negative) sectional curvature equal to  $-1$ . This means that geodesics between two points of  $H^n$  are unique. Moreover,  $H^n$  is simply connected.

The Poincare disc  $\mathbb{D}$  is a model of two-dimensional hyperbolic geometry  $H^2$ . It is defined as the disc  $\{z = x + iy \in \mathbb{C} : |z| < 1\}$ , with the hyperbolic metric

$$ds^2 = \frac{dx^2 + dy^2}{(1 - x^2 - y^2)^2}.$$

The hyperbolic distance between two points  $x, y \in \mathbb{D}$ , denoted by  $d_{\mathbb{D}}(x, y)$  is given by

$$\frac{1}{2}(\cosh(d_{\mathbb{D}}(x, y)) - 1) = \frac{|x - y|^2}{(1 - |x|^2)(1 - |y|^2)}.$$

In  $\mathbb{D}$ , a line is represented as an arc of a circle whose ends are perpendicular to the disk's boundary (and diameters are also permitted). Two arcs which do not meet correspond to parallel rays, arcs which meet orthogonally correspond to perpendicular lines, and arcs which meet on the boundary are a pair of limits rays.

$\mathbb{D}$  admits certain transformations called *Mobius Transformations*  $F : \mathbb{D} \rightarrow \mathbb{D}$ , given by

$$F(z) = \frac{\alpha z + \beta}{\beta^* z + \alpha^*},$$

where  $\alpha^* \alpha - \beta^* \beta = 1$ . Each Mobius transformation can be represented by a matrix

$$F = \begin{pmatrix} \alpha & \beta \\ \beta^* & \alpha^* \end{pmatrix}.$$

Such transformations together with the conjugate map  $C(z) = z^*$  make the *general Mobius group* of transformations, denoted by  $M(\mathbb{D})$ .

#### 2) Tessellation of the Poincare disc by Schottky groups:

Let us now describe a tessellation or packing of  $\mathbb{D}$  by means of certain Mobius transformations that act as group actions on  $\mathbb{D}$ . We will see later how to use this construction for describing a quotient space which is homeomorphic to  $\mathcal{T}$ .

Let  $C_i, C'_i, 1 \leq i \leq k$  be a set of  $2n$  circles in  $\mathbb{C}$  such that the interiors of the  $2k$  circles are all pairwise disjoint. Let  $\mathcal{F}$

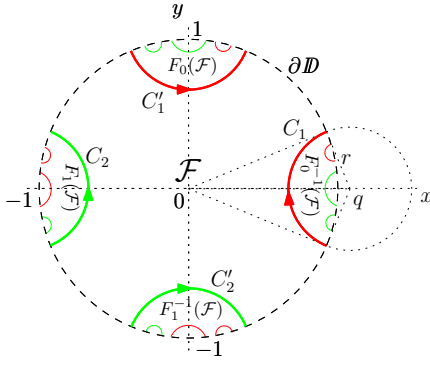


Fig. 5. The Schottky domain  $\mathcal{F} \subset \mathbb{D}$  and the pairings  $C_1, C_1', C_2, C_2'$ , depicted by the thicker circles in red and green. The Möbius transformations respect the identifications on the circles. The smaller circles (along with  $C_i', C_i$ ), bound the images of the transformations  $F_0, F_1, F_0^{-1}, F_1^{-1}$  on  $\mathcal{F}$ .

be the intersection of the exteriors of these circles.  $\mathcal{F}$  is called a (classical) *Schottky domain*. A *Schottky pairing* is a set of  $k$  Möbius transformations,  $F_1, \dots, F_k$ , where each  $F_i$  maps the exterior of  $C_i$  onto the interior of  $C_i'$ .  $\{F_i\}$  are called the side pairings. The group generated by the side-pairing is called a (classical) Schottky group on the generators  $F_1, \dots, F_k$ . The following results are known about these groups.

**Theorem 3.1:** [5] Let  $\Gamma$  be a classical Schottky subgroup of  $M(\mathbb{D})$  of rank  $m$  corresponding to a Schottky domain  $\mathcal{F}$ . Then :

- 1)  $\Gamma$  is a free subgroup of  $M(\mathbb{D})$  of rank  $m$ .
- 2) If no two sides of  $\mathcal{F} \subset \mathbb{D}$  meet at infinity, then the space produced by the side-pairings of  $\mathcal{F}$  is the same as  $\mathbb{D}/\Gamma$ .

The action of Schottky groups on  $\mathbb{D}$  results in a space  $\mathbb{D}/\Gamma$  by gluing together together the sides of the Schottky domain via the Schottky pairings. Since the action is free, this produces a packing of  $\mathbb{D}$ . The limit points (on  $\partial\mathbb{D}$ ) of these group actions have interesting properties. If we let  $L(\Gamma) \subset \partial\mathbb{D}$  be the set of all limit points, then we have the following result.

**Theorem 3.2:** [5] Let  $\Gamma$  be a Schottky group generated by a Schottky pairing of a Schottky domain with at least four sides and in which no two sides meet at  $\partial\mathbb{D}$ . Then  $L(\Gamma)$  is a Cantor set.

We now present one particular construction. Let  $q \in \mathbb{C}$  be the center of a circle of radius  $r$  in  $\mathbb{C}$  given by the equation  $(z - q)^*(z - q) = r^2$ . Let this circle cut the unit circle (identified with  $\partial\mathbb{D}$ ) perpendicularly, as illustrated in Figure 5. Let  $q$  be parameterized by

$$q = \frac{\cosh(x_0)}{\sinh(x_0)} \exp(i\alpha).$$

As shown in [4], the transformation, given by

$$G_q := \begin{pmatrix} i \cosh(x_0) \exp(i\alpha) & -i \sinh(x_0) \\ i \sinh(x_0) & -i \cosh(x_0) \exp(-i\alpha) \end{pmatrix},$$

is a Möbius transformation on  $\mathbb{D}$ , where  $x_0 = \sinh^{-1}(1/r)$ . This transformation produces a reflection about the circle

at center  $q$  and radius  $r = \sqrt{|q|^2 - 1}$ . It is an isometry in which all points on the circle centered at  $q$  remain fixed. Furthermore, the points outside this circle are mapped to its interior and vice versa.

Now construct a Schottky domain using four circles of equal radius  $C_1, C_1', C_2, C_2'$  centered at four symmetric points  $q_0, q_1, q_2, q_3$  on the axes. In order to keep the circles from intersecting, the radii should satisfy  $0 < r < 1$ . This means that  $\sinh^{-1}(1) < x_0 < \infty$ . Therefore, the Schottky domain is formally defined by

$$\mathcal{F} = \{z \in \mathbb{D} : (z - q_k)^*(z - q_k) < r^2, k = 0, 1, 2, 3\},$$

where

$$q_k = \frac{\cosh(x_0)}{\sinh(x_0)} \exp(ik\pi/2), k = 0, 1, 2, 3;$$

$$r = \sqrt{(\cosh(x_0)/\sinh(x_0))^2 - 1}.$$

We now define the Schottky (free) group  $\Gamma$  generated by two transformations  $F_0, F_1 \in M(\mathbb{D})$ , where

$$F_0(z) = \exp(i\pi/2)G_{q_0}(z^*),$$

$$F_1(z) = \exp(i\pi/2)G_{q_2}(z^*).$$

Note that  $z \mapsto z^*$  is a reflection about the  $y$ -axis and the multiplication factor  $\exp(i\pi/2)$  is a  $90^\circ$  anticlockwise rotation. Therefore,  $F_0$  maps the exterior of  $C_1$  to the interior of  $C_1'$ . Similarly,  $F_1$  maps the exterior of  $C_2$  to the interior of  $C_2'$ . This satisfies the pairing property of the Schottky domain.

By Theorem 3.1,  $\Gamma$  is a free group generated by two generators  $F_0, F_1$ . In other words, any member of  $\Gamma$  can be written as a composition  $g_1 g_2 \dots g_k$ , where  $g_i \in \{F_0, F_1, F_0^{-1}, F_1^{-1}\}$ . The set  $\{g(\mathcal{F}) : g \in \Gamma\}$ , is a packing or tessellation of  $\mathbb{D}$ . The free action of  $\Gamma$  ensures that the orbits of  $\mathcal{F}$  cover the entire disc  $\mathbb{D}$  in the limit. An incomplete picture of this tessellation can be seen in Figure 5. The members of  $\Gamma$  produce images of  $\mathcal{F}$  with an infinite detail. The limit set  $L(\Gamma) \subset \partial\mathbb{D}$  is fractal as predicted by Theorem 3.2. By Theorem 3.1, the space  $\mathbb{D}/\Gamma$  is exactly the space described by the identification of the Schottky domain by the side-pairings. Thus  $\mathbb{D}$  is a universal cover of this space.

We add one final modification to our construction. Consider the space  $\mathbb{D} \times (0, 1)$  as a 'fat' Poincare Disc. Also let the set  $\mathcal{F} \times (0, 1)$  be acted upon by the group of transformations  $\bar{\Gamma} : \mathbb{D} \times (0, 1) \rightarrow \mathbb{D} \times (0, 1)$ , whose members  $\bar{g}$  are defined by

$$\bar{g}(z, t) = (g(z), t), g \in \Gamma.$$

Thus  $\bar{\Gamma}$  produces a (fat) tessellation of the space  $\mathbb{D} \times (0, 1)$ . This has been illustrated in Figure 6.

Returning to the space  $S^1 \vee S^1$  introduced in the previous section, we can see that  $\mathbb{D}/\Gamma$  is a planar thickening of  $S^1 \vee S^1$ . We also noted that its universal cover  $\bar{X}$  is a fractal set in  $\mathbb{R}^2$  and a thickening of  $S^1 \vee S^1$  produces a thickening of its universal cover as well. It is easy to see now that in the construction presented above, the boundary (in the limit) of this thickened fractal object has been mapped onto  $L(\Gamma)$  so that the resulting space  $\mathbb{D}$  is another representation of

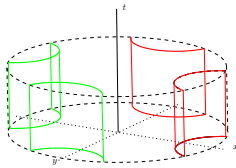


Fig. 6. The space  $\mathbb{D} \times (0, 1)/\bar{\Gamma}$ . The group  $\bar{\Gamma}$  acts on  $\mathcal{F} \times (0, 1)$  bounded by red and green surfaces in  $\mathbb{D} \times (0, 1)$  to produce a (fat) tiling so that  $\mathbb{D} \times (0, 1)$  is the universal cover.

the universal cover. By the modification discussed above, it can be seen readily that the space  $\mathbb{D} \times (0, 1)/\bar{\Gamma}$  is (upto homeomorphism) the solid double torus  $\mathbf{T}^2$ , introduced previously as the topology of the configuration space  $\mathcal{T}$ . Note also that

$$\pi_1(\mathbb{D} \times (0, 1)) \cong \pi_1(S^1 \vee S^1) \cong \mathbb{Z} * \mathbb{Z} \cong \bar{\Gamma}.$$

Thus we have state our main result.

*Theorem 3.3:*  $H^2 \times (0, 1)$  is a universal covering space of the solid double torus  $\mathbf{T}^2$ .

For the purpose of calculation we restate that  $\mathbb{D} \times (0, 1)$  is a universal cover of  $\mathcal{T}$ . All we need is an explicit homeomorphism between  $\mathcal{F} \times (0, 1)$  and a corresponding fundamental domain in  $\mathcal{T}$ . If we introduce a metric on  $\mathbb{D} \times (0, 1)$  given by

$$ds^2 = \frac{dx^2 + dy^2}{(1 - x^2 - y^2)^2} + dt^2,$$

the geodesics on this covering space can be computed. These geodesics, when projected back to the quotient space provide motion planning strategies for  $\mathcal{T}$  via the maps constructed below.

### B. Construction of Homeomorphisms

We now outline briefly the explicit maps that provide the homeomorphism between the fundamental domain of the actual configuration space  $\mathcal{T}$  and  $\mathcal{F} \times (0, 1)$ . The full details of these maps will be given in a future work.

As a first step, we need a map that inverts the constraint  $r_1^2 + r_2^2 - 2r_1r_2 \cos(\theta) < R_c^2$  (See Figure 2), so that the space is a rectangular open column bounded by the planes  $r_1 > 0, r_2 > 0, r_1 < R_c, r_2 < R_c$  and identified at the planes where  $\theta$  equal to  $\pi$  and  $-\pi$ . We omit the details of this map for the sake of brevity. We note however, that the cylindrical void due to the collision constraints is still preserved.

Next we obtain the fundamental domain of the space by two cuts at the  $\theta = 0$  plane. These cuts split the cylindrical void into two and results in a (simply connected) fundamental domain of  $\mathcal{T}$ . This has been depicted in Figure 7. Now take a family of rectangular sections of this column by varying  $r_1$  from  $R_o$  to  $R_c$ . A typical section would resemble the left most picture in Figure 8, with  $R_o$  exaggerated for illustration. Figure 8 pictorially portrays how to map each rectangular section to  $\mathcal{F}$  inside  $\mathbb{D}$ . The construction of these maps is quite straightforward and we omit the details due to the lack of space. As  $r_1$  varies over  $(R_o, R_c)$ , each rectangular section is mapped onto the set

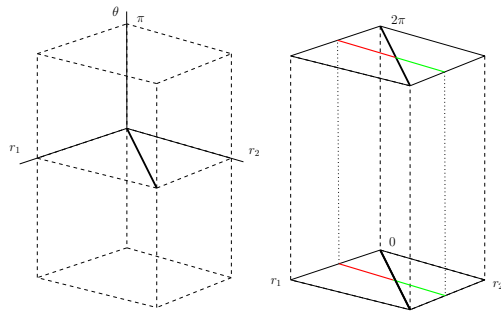


Fig. 7. The configuration space  $\mathcal{T}$  after the correction of communication constraints (left) and its fundamental domain (right).

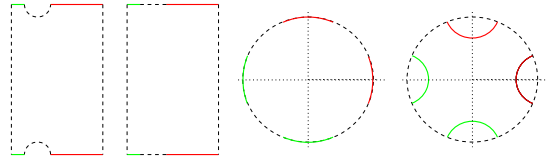


Fig. 8. A series of maps between a rectangular section in the fundamental domain of  $\mathcal{T}$  and the Schottky domain  $\mathcal{F} \subset \mathbb{D}$ .

$\mathcal{F} \times \{(r_1 - R_o)/(R_c - R_o)\}$  in  $\mathbb{D} \times (0, 1)$ . We have omitted the minor details on how to deal with the sections when  $r_1$  is close to  $R_o$  and  $R_c$ .

## IV. CONCLUSIONS AND FUTURE WORK

In this paper, we have focussed on the motion planning problem on one particular configuration space that has the topology of a solid double torus. The technique of constructing the universal cover of the configuration space has been found to be useful for the solution to this problem. We point out here that although this construction looks specific to one particular sensor arrangement for a certain number of agents, the techniques can be employed for various other scenarios.

It is evident from a preliminary study of the configuration spaces of sensor arrangements for a larger number of agents that their topologies are handle-bodies of higher genus and the explicit construction of their universal cover would need similar techniques from hyperbolic geometry. Finally, we want to understand the configuration spaces for robotic sensor network with arbitrary connectivity.

### ACKNOWLEDGEMENTS

The author would like to thank Dr. Daniel Koditschek for many fruitful discussions during the course of this work.

### REFERENCES

- [1] B. Donald, "Information invariants in robotics," *Artificial Intelligence* Vol. 72, pp. 217-304, 1995.
- [2] B. Tovar, A. Yershova, J. O'Kane, and S. LaValle, "Information spaces for mobile robots," in *Proc. International Workshop on Robot Motion and Control*, 2005.
- [3] A. Hatcher, *Algebraic Topology*, Cambridge University Press, 2002.
- [4] J. Magnus, *Non-Euclidean Tessellations and Their Groups*, Academic Press, New York, 1974.
- [5] J. Ratcliffe, "Foundations of Hyperbolic Manifolds", Springer-Verlag, 1994.
- [6] E. Rimon and D. E. Koditschek, "Exact robot navigation using artificial potential functions," *IEEE Transactions on Robotics and Automation*, Vol. 8(5), pp. 501-518, October 1992.